Inorganica Chimica Acta 376 (2011) 278–284

Contents lists available at ScienceDirect

Inorganica Chimica Acta

journal homepage: www.elsevier.com/locate/ica

Versatile coordination behavior of *N,N*-di(alkyl/aryl)-*N′*-benzoylthiourea ligands: Synthesis, crystal structure and cytotoxicity of palladium(II) complexes

N. Selvakumaran [a], Seik Weng Ng [b], Edward R.T. Tiekink [b], R. Karvembu [a,*]

[a] Department of Chemistry, National Institute of Technology, Tiruchirappalli 620015, India
[b] Department of Chemistry, University of Malaya, 50603 Kuala Lumpur, Malaysia

ARTICLE INFO

Article history:
Received 8 March 2011
Received in revised form 10 June 2011
Accepted 16 June 2011
Available online 23 June 2011

Keywords:
Palladium(II)
Thiourea
Synthesis
X-ray structures
Anti-cancer activity

ABSTRACT

The synthesis and characterization of Pd(II) complexes with the general formula *cis*-[Pd(L-O,S)$_2$] (HL = *N,N*-diethyl-*N′*-benzoylthiourea, *N,N*-diisobutyl-*N′*-benzoylthiourea or *N,N*-dibenzyl-*N′*-benzoylthiourea) and *trans*-[PdCl$_2$(HL-S)$_2$] (HL = *N,N*-diphenyl-*N′*-benzoylthiourea, *N,N*-di-*n*-butyl-*N′*-benzoylthiourea or *N,N*-diisopropyl-*N′*-benzoylthiourea) are reported. These complexes were formed from the reaction between PdCl$_2$ and *N,N*-di(alky/aryl)-*N′*-benzoylthiourea in acetonitrile with the formulation dependent on the nature of HL. The new Pd(II) complexes have been characterized by analytical and spectral (FT-IR, UV–Vis, ^{1}H NMR and ^{13}C NMR, Mass) techniques. The molecular structures of two of the complexes (**1** and **5**) have been conformed by X-ray crystallography. Complex **1** shows cytotoxicity against human breast cancer cells.

1. Introduction

We are currently interested in the coordination chemistry of *N,N*-di(alkyl/aryl)-*N′*-benzoylthiourea ligands (Fig. 1) in view of their interesting and versatile coordination behavior towards transition metals [1,2]. Three different coordination modes have been found so far for this type of ligand in their mononuclear transition metal complexes. They are monobasic bidentate (O,S) [3], neutral monodentate (S) [4] and neutral bidentate (O,N) [5]. Among these, monobasic bidentate (O,S) coordination is very common and leads to stable Pd(II) [6,7], Cu(II) [8], Pt(II) [9,10], Co(III) [10], Rh(III) [11], Ni(II) [10,12] and Co(II) [12] complexes. On the other hand, coordination through S only is rare and observed in few transition metal complexes. When present, the monodentate coordination was explained on the basis of intramolecular hydrogen bond formation between the carbonyl O atom and the thiourea NH group (Fig. 2) [13]. This is true in their Pt(II) [14], Pd(II) [13], Cu(I) [15] and Cd(II) [16] complexes. There are very few reports in which *N,N*-di(alkyl/aryl)-*N′*-benzoylthiourea ligands that is without the thiourea NH moiety, where coordinated to the metal is through S only [17,18]. The reaction between Pd(II) salts and *N,N*-di(alkyl/aryl)-*N′*-benzoylthiourea ligands (HL) have so far yielded only complexes of the type *cis*-[Pd(L-O,S)$_2$] [6–8]. Interestingly, we were able to obtain Pd(II) complexes of the type *cis*-[Pd(L-O,S)$_2$] or *trans*-[Pd(HL-S)$_2$] when reaction was carried out between PdCl$_2$ and *N,N*-di(alkyl/aryl)-*N′*-benzoylthiourea ligand. *N,N*-di(ethyl/isobutyl/benzyl)-*N′*-benzoylthiourea ligands gave *cis*-[Pd(L-O,S)$_2$] and *N,N*-di(phenyl/n-butyl/isopropyl)-*N′*-benzoylthiourea ligands formed *trans*-[PdCl$_2$(HL-S)$_2$] on reaction with PdCl$_2$ in acetonitrile. It was already realized that *N*-substituents can influence the coordination mode of ligand; for example, coordination of dimethyl substituted ferrocene carbonyl thiourea (HL′) to Cu(II) ion differed substantially from that of the corresponding diethyl substituted analog (HL″). The former yielded a bis-sulfur bridged Cu(II) dimer, [{CuL′(HL′)Cl}$_2$] [17] while the latter only coordinated in a bidentate manner to yield a single mononuclear Cu(II) complex [CuL″$_2$] [19].

N,N-Di(alkyl/aryl)-*N′*-benzoylthiourea ligands were effectively utilized for liquid–liquid extraction of the platinum group metals from hydrochloric acid solutions [20–23]. The determination of traces of the platinum group metals by means high performance thin layer chromatography (HPTLC) after complexation with suitably modified fluorescent *N*-aroylthiourea has also been of interest [24–27]. Recently *N,N*-diethyl-*N′*-benzoylthiourea has been used for the selective online preconcentration and highly selective trace determination of Pd(II) by means of graphite furnace atomic absorption spectroscopy [28].

Transition metal complexes with thiourea derivatives are also known to exhibit a wide range of biological activities such as antiviral, antibacterial, antifungal, anticancer, antitubercular, antithyroidal, insecticidal, antimalarial, etc. [29–33]. *N*-Substituents not only influenced the coordination behavior of ligands but also the chemical and physical properties of its complexes. Indeed cytotoxicity

* Corresponding author. Tel.: +91 4312503636; fax: +91 431 2500133.
E-mail address: kar@nitt.edu (R. Karvembu).

0020-1693/$ - see front matter © 2011 Elsevier B.V. All rights reserved.
doi:10.1016/j.ica.2011.06.031

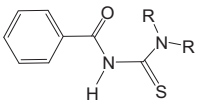

R	Abbreviation
C_2H_5	HL1
$(CH_3)_2CHCH_2$	HL2
$C_6H_5CH_2$	HL3
C_6H_5	HL4
$CH_3(CH_2)_3$	HL5
$(CH_3)_2CH$	HL6

Fig. 1. Structure of *N*,*N*-di(alkyl/aryl)-*N*′-benzoylthiourea ligands.

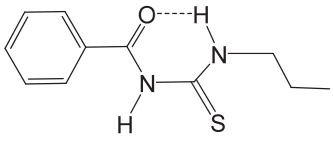

Fig. 2. Structure of *N*-benzoyl-*N*′-propylthiourea containing thiourea NH moiety which forms an intramolecular hydrogen bond with the proximate carbonyl atom (indicated by dashed line).

studies using HeLa cancer cell lines have demonstrated that some of the platinum acylthioureas showed cytotoxicity behavior with their antiproliferative effects being dependent on the nature/type of the substituent on the acyl thiourea ligand [9]. On the basis of the structural and thermodynamic analogy between Pt(II) and Pd(II) complexes [34–38], there is also much interest in the design and synthesis of Pd(II) derivatives capable of interacting with biomolecules producing a pharmacological action [39]. Furthermore, some mixed ligand Pd(II) complexes have been shown to act as potential anticancer agents [40–47]. In this context, we have also studied anticancer activity of Pd(II) complexes containing *N*,*N*-di(alkyl/aryl)-*N*′-benzoylthiourea ligand.

2. Experimental

2.1. Materials and physical measurements

$PdCl_2$ and ligand precursors were of reagent grade and used without further purification. The *N*,*N*-di(alkyl/aryl)-*N*′-benzoylthiourea derivatives were prepared according to previously published method [1,2]. The solid state IR spectra were recorded in the range 4000–400 cm^{-1} on a PerkinElmer FT-IR spectrophotometer with KBr pellets. All the ^1H and ^{13}C NMR spectra were recorded, using $CDCl_3$ as solvent and TMS as internal standard on a Bruker 400 MHz NMR spectrometer. MALDI-TOF mass spectrometry experiments were performed on a 4800-Applied Bio System mass spectrometer, using TiO_2 as matrix. Electronic spectra of the complexes were recorded on a T90 + PG instruments UV–Vis spectrophotometer using dichloromethane as a solvent.

2.2. Synthesis of cis-[Pd(L1-O,S)$_2$] (**1**)

Ligand (HL1) (0.284 g, 1.2 mmol) dissolved in acetonitrile (20 ml) was added drop wise to an acetonitrile solution (20 ml) of $PdCl_2$ (0.106 g, 0.6 mmol) at room temperature and the resulting mixture was stirred for 5 h. The red crystalline precipitate that formed was filtered and washed with diethyl ether and then dried in vacuum. Crystals of suitable quality for X-ray diffraction studies were obtained by slow evaporation of its dichloromethane solution. Yield: 76%. m.p.: 134 °C. *Anal.* Calc. for $C_{24}H_{30}N_4O_2PdS_2$: C, 49.96; H, 5.24; N, 9.71; S, 11.11. Found: C, 49.45; H, 4.97; N, 9.45; S, 11.02%. IR (KBr) ν/cm^{-1}: 1585 (νC⎓O), 1247 (νC⎓S). UV–Vis (CH_2Cl_2) λ_{max} (nm) ($\varepsilon/dm^3\,mol^{-1}\,cm^{-1}$): 274 (74 383), 240 (51 486). ^1H (400 MHz, $CDCl_3$) δ (ppm): 1.28–1.32 (t, J = 8.0 Hz, 12H, CH_3), 3.83–3.87 (m, 8H, CH_2), 7.39–8.30 (m, 10H, aromatic). ^{13}C NMR (400 MHz, $CDCl_3$) δ (ppm): 12.6, 13.1, 46.1, 47.2, 127.9, 129.6, 131.5, 137.1, 170.6, 171.0. MS (MALDI) *m/z* 616.95 [(**1**) K]$^+$.

2.3. Synthesis of cis-[Pd(L2-O,S)$_2$] (**2**)

Complex **2** was prepared by a similar procedure as described for **1** from HL2 (0.351 g, 1.2 mmol) and $PdCl_2$ (0.106 g, 0.6 mmol). Yield: 87%. m.p.: 153 °C. *Anal.* Calc. for $C_{32}H_{46}N_4O_2PdS_2$: C, 55.76; H, 6.73; N, 8.13; S, 9.30. Found: C, 55.34; H, 6.48; N, 7.98; S, 9.04%. IR (KBr) ν/cm^{-1}: 1586 (νC⎓O), 1230 (νC⎓S). UV–Vis (CH_2Cl_2) λ_{max} (nm) ($\varepsilon/dm^3\,mol^{-1}\,cm^{-1}$): 276 (58 334), 241 (42 575). ^1H NMR (400 MHz, $CDCl_3$) δ (ppm): 0.91–0.99 (d, J = 8.0 Hz, 24H, CH_3), 2.26–2.29 (m, 4H, CH), 3.64–3.68 (m, 8H, CH_2), 7.41–8.25 (m, 10H, aromatic). ^{13}C NMR (400 MHz, $CDCl_3$) δ (ppm): 20.3, 20.4, 27.4, 27.7, 60.3, 61.2, 127.9, 129.6, 131.4, 137.0, 170.3, 172.3. MS (MALDI) *m/z* 689.13 [M]$^+$.

2.4. Synthesis of cis-[Pd(L3-O,S)$_2$] (**3**)

Complex **3** was prepared by a similar procedure as described for **1** from HL4 (0.433 g, 1.2 mmol) and $PdCl_2$ (0.106 g, 0.6 mmol). Yield: 77%. m.p.:198 °C. *Anal.* Calc. for $C_{44}H_{38}N_4O_2PdS_2$: C, 64.03; H, 4.64; N, 6.79; S, 7.77. Found: C, 63.95; H, 4.36; N, 6.45; S, 7.44%. IR (KBr) ν/cm^{-1}: 1541 (νC⎓O) 1251 (νC⎓S). UV–Vis (CH_2Cl_2) λ_{max} (nm) ($\varepsilon/dm^3\,mol^{-1}\,cm^{-1}$): 278 (69 199), 240 (44 482). ^1H NMR (400 MHz, $CDCl_3$) δ (ppm): 5.04 (s, 4H, CH_2), 5.13 (s, 4H, CH_2), 7.28–7.52 (m, 36, aromatic), 8.23 (d, J = 7.2 Hz, 4H, aromatic), ^{13}C NMR (400 MHz, $CDCl_3$) δ (ppm): 52.4, 54.5, 127.7, 136.8, 172.1, 174.2. MS (MALDI) *m/z* 864.98 [M]$^+$.

2.5. Synthesis of trans-[PdCl$_2$(HL4-S)$_2$] (**4**)

Complex **4** was prepared by a similar procedure as described for **1** from HL4 (0.399 g, 1.2 mmol) and $PdCl_2$ (0.106 g, 0.6 mmol). Yield: 78%. m.p.: 190 °C. *Anal.* Calc. for $C_{40}H_{32}N_4O_2Cl_2PdS_2$: C, 57.05; H, 3.83; N, 6.65; S, 7.60. Found: C, 56.89; H, 3.67; N, 6.45; S, 7.47%. IR (KBr) ν/cm^{-1}: 3415 (νN–H), 1699 (νC═O), 1243 (νC═S). UV–Vis (CH_2Cl_2) λ_{max} (nm) ($\varepsilon/dm^3\,mol^{-1}\,cm^{-1}$): 284 (52 184), 228 (52 923). ^1H NMR (400 MHz, $CDCl_3$) δ (ppm): 7.30–7.34 (m, 20H, aromatic), 7.37–7.77 (m, 10H, aromatic), 11.95 (s, 2H, NH). ^{13}C NMR (400 MHz, $CDCl_3$) δ (ppm): 128.9, 129.6, 134.5, 137.1, 164.2, 170.3. MS (MALDI) *m/z* 808.93 [M]$^+$.

2.6. Synthesis of [trans-[PdCl$_2$(HL5-S)$_2$] (**5**)

Complex **5** was prepared by a similar procedure as described for **1** from HL5 (0.351 g, 1.2 mmol) and $PdCl_2$ (0.106 g, 0.6 mmol). Yield: 72%. m.p.:148 °C. *Anal.* Calc. for $C_{32}H_{48}Cl_2N_4O_2PdS_2$: C, 50.43; H, 6.35; N, 7.35; S, 8.41. Found: C, 50.10; H, 6.09; N, 7.01; S, 8.28%. IR (KBr) ν/cm^{-1}: 3120 (νN–H), 1694 (νC═O), 1251 (νC═S), UV–Vis (CH_2Cl_2) λ_{max} (nm) ($\varepsilon/dm^3\,mol^{-1}\,cm^{-1}$): 275 (65 926), 240 (48 098). ^1H NMR (400 MHz, $CDCl_3$) δ (ppm): 0.99–1.18 (t, J = 7.2 Hz, 12H, CH_3), 1.19–1.46 (m, 8H, CH_2), 1.59–1.82 (m, 8H, CH_2), 3.43–3.87 (m, 8H, CH_2), 7.41–8.12 (m, 10H, C_6H_5), 11.4 (s,

2H, NH). ^{13}C NMR (400 MHz, $CDCl_3$) δ (ppm): 13.1, 13.8, 20.1, 20.3, 28.6, 29.7, 55.2, 53.4, 128.9, 129.1, 131.4, 133.5, 163.4, 178.2.

2.7. Synthesis of trans-[$PdCl_2$(HL6-S)$_2$] (**6**)

Complex **6** was prepared by a similar procedure as described for **1** from HL6 (0.317 g, 1.2 mmol) and $PdCl_2$ (0.106 g, 0.6 mmol). Yield: 82%. m.p.: 126 °C. *Anal.* Calc. for $C_{28}H_{40}N_4O_2Cl_2PdS_2$: C, 47.63; H, 5.71; N, 7.94; S, 9.08. Found: C, 47.38; H, 5.45; N, 7.58; S, 8.87%. IR (KBr) ν/cm^{-1}: 3164 (νN–H), 1677 (νC=O), 1266 (νC=S). UV–Vis (CH_2Cl_2) λ_{max} (nm) (ε/dm^3 mol^{-1} cm^{-1}): 278 (61 323), 244 (44 268). ^{1}H NMR (400 MHz, $CDCl_3$) δ (ppm): 1.28–1.72 (m, 24H, CH_3), 4.39–4.40 (m, 4H, CH), 7.30–8.03 (m, 10H, C_6H_5), 11.3 (s, 2H, NH). ^{13}C NMR (400 MHz, $CDCl_3$) δ (ppm): 20.2, 21.1, 54.3, 54.8, 128.1, 128.9, 129.20, 130.1, 164.4, 170.4.

Table 1
Crystal data for **1** and **5**.

Crystal data	**1**	**5**
Empirical formula	$C_{24}H_{30}N_4O_2PdS_2$	$C_{32}H_{48}Cl_2N_4O_2PdS_2$
Formula weight	577.04	762.16
Crystal color	red	red
Crystal dimensions (mm)	0.20 × 0.30 × 0.40	0.20 × 0.25 × 0.30
Crystal system	monoclinic	monoclinic
Lattice type	primitive	primitive
Space group	$P2_1/n$	$P2_1/c$
a (Å)	10.2394(5)	11.0344(3)
b (Å)	18.4336(9)	17.3072(5)
c (Å)	13.2898(7)	9.4781(3)
β (°)	105.138(1)	93.878(3)
V (Å^3)	2421.4(2)	1805.93(9)
Z	4	2
D_x (g cm^{-3})	1.583	1.402
F(0 0 0)	1184	792
μ (Mo Kα) (mm^{-1})	0.968	0.968
Temperature (K)	100(2)	295(2)
Reflections collected	22 469	9254
R_{int}	0.023	0.027
Unique reflections	5562	4026
Obs. reflections [$I > 2\sigma(I)$]	5133	3059
R (Obs. reflections)	0.022	0.039
a, b, in weighting scheme	0.029, 2.089	0.047, 0.764
wR (all data)	0.058	0.106

2.8. X-ray crystallography

Crystals of **1** and **5** suitable for X-ray diffraction were grown from their respective dichloromethane solutions. X-ray diffraction measurements of **1** and **5** were performed on a Bruker SMART APEX-II CCD diffractometer and Agilent Supernova dual diffractometer with Atlas (Mo) detector, respectively, using graphite monochromatized Mo Kα radiation so that θ_{max} was 27.5°. Crystal data are given in Table 1. The structures were solved by direct-methods (SHELXS-86 [48]) and refined (anisotropic displacement parameters, H atoms in the riding model approximation and a weighting scheme of the form $w = 1/[\sigma^2(F_o^2) + aP^2 + bP]$ where $P = (F_o^2 + 2F_c^2)/3$) with SHELXL-97 on F^2 [48]. The molecular structures are shown in Figs. 3 and 4 which were drawn with displacement ellipsoids at the 70% probability level [49]. The crystal packing diagrams were drawn with DIAMOND [50] using arbitrary spheres.

2.9. Cell culture

MCF 7 (human breast cancer cell line, NCCS Pune) and L929 (mouse fibroblast cell line, NCCS Pune) were maintained in minimum essential medium (MEM) supplemented with 10% fetal bovine serum (FBS). The cells were incubated in CO_2 incubator with 5% CO_2. After attaining confluency, the cells were detached from the flask with Trypsin-EDTA. The cell suspension was centrifuged at 3000 rpm for 3 min and then re-suspended in the growth medium for further studies.

2.10. Cytotoxicity experiments

For cytotoxicity experiments, L929 and MCF7 were seeded on a 96 well plate with a density of 10 000 cells/cm^2. MTT [3-(4,5-dimethylthiazole-2-yl)-2,5-diphenyltetrazolium] assay was used to evaluate cytotoxicity of the HL1 and **1**. This is a colorimetric test based on the selective ability of viable cells to reduce the tetrazolium component of MTT into purple colored formazan crystals. Three different concentrations of the samples (1, 5 and 10 mg/ml) were prepared by dilution with the media. After attaining 90% confluency, the cells were washed with phosphate buffer saline (PBS) and the compounds of different concentrations (100 µl)

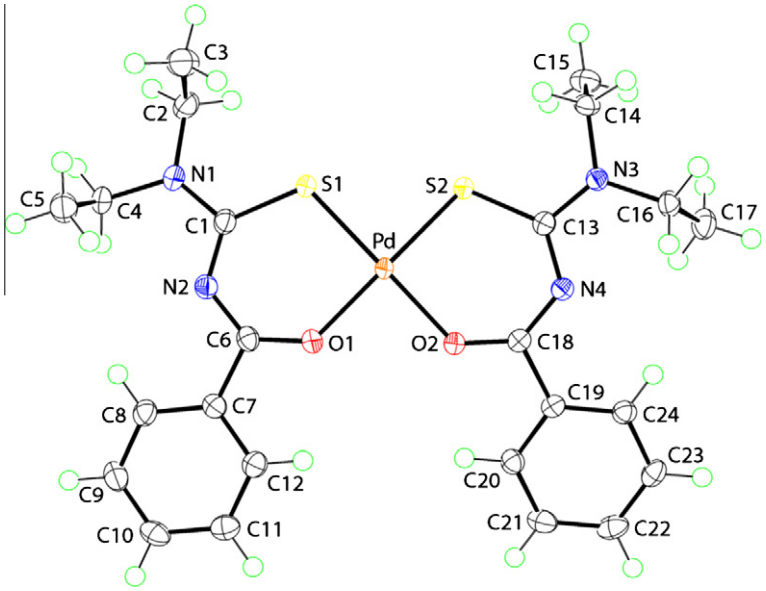

Fig. 3. Molecular structure of **1** showing atomic labeling scheme.

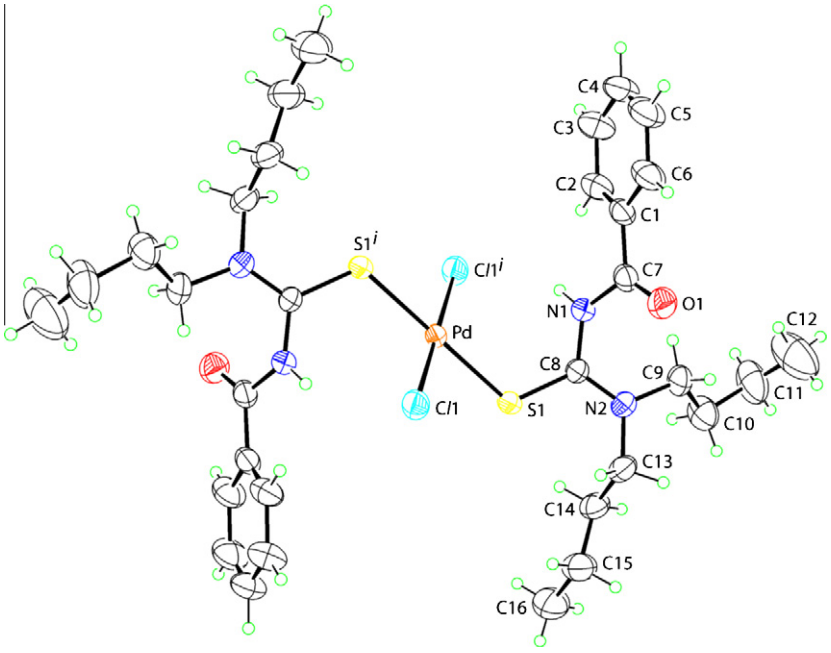

Fig. 4. Molecular structure of **5** showing atomic labeling scheme. The primed atoms are related by the symmetry operation $1 - x, 1 - y, 1 - z$.

were added and incubated. Cells in media alone devoid of compound acted as negative control and wells treated with Triton X-100 as positive control for a period of 24 h. 5 mg of MTT (Sigma) was dissolved in 1 ml of PBS and filter sterilized. 10 μl of the MTT solution was further diluted to 100 μl with 90 μl of serum and phenol red free medium. The cells were incubated with 100 μl of the above solution for 4 h to form formazan crystals by mitochondrial dehydrogenases. 100 μl of the solubilization solution (10% Triton X-100, 0.1 N HCl and isopropanol) was added in each well and incubated at room temperature for 1 h to dissolve the formazan crystals. The optical density of the solution was measured at a wavelength of 570 nm using a Beckmann Coulter Elisa plate reader (BioTek Power Wave XS). Triplicate samples were analyzed for each experiment.

3. Results and discussion

The present work deals with the synthesis and characterization of two different kinds of Pd(II) complexes. Reactions of $PdCl_2$ with HL1, HL2 or HL3 in acetonitrile gave square planar complexes of the type *cis*-[Pd(L-O,S)$_2$] while similar reactions with HL4, HL5 or HL6 resulted in square planar complexes of the type *trans*-[$PdCl_2$(HL-S)$_2$] (Scheme 1). The molar ratio of $PdCl_2$ and ligand was 1:2 in each case. The complexation reaction was highly selective in the sense that only one product was formed in each reaction. The structures of the complexes were confirmed by analytical, spectral and X-ray diffraction studies. The Pd(II) complexes were also subjected to anticancer activity studies. All the complexes are air stable and soluble in common organic solvents such as $CHCl_3$, CH_2Cl_2, DMSO and DMF.

3.1. IR spectra

The bands at 1652, 1687 and 1689 cm^{-1} in the IR spectra of HL1, HL2 and HL3, respectively can be assigned to the C═O stretching mode of the carbonyl group, which shifted to the lower wave number (1541–1586 cm^{-1}) upon complexation in **1**, **2** and **3**. A thionyl (C═S) vibration band which appeared in the IR spectra of ligands (1311–1263 cm^{-1}) similarly underwent a shift into lower frequency (1251–1225 cm^{-1}) in their Pd(II) complexes. The NH stretching vibration in the range 3328–3260 cm^{-1} for HL1, HL2 and HL3 disappeared in their Pd(II) complexes. The IR data indicates that each ligand underwent enolization followed by deprotonation prior to coordination to Pd(II) ion through O and S atoms. The IR spectra of **4**, **5** and **6** showed the following significant changes when compared with the spectra of corresponding ligands (HL4, HL5 and HL6). The C═S stretching frequency observed in the region 1355–1282 cm^{-1} in the IR spectra of free ligands shifted to lower frequency (1267–1205 cm^{-1}) in their complexes. For free ligands, the stretching frequency in the region 1691–1650 cm^{-1}, assigned to the carbonyl moiety, was unaltered in their complexes indicating non participation of carbonyl oxygen in coordination. Finally, the NH stretching in the ligands (3383–3174 cm^{-1}) is also present in the same region in the corresponding Pd(II) complexes indicating that enolization and deprotonation did not occur. The IR data revealed that in **4**, **5** and **6**, the thiourea derivatives are coordinated through the S atom only.

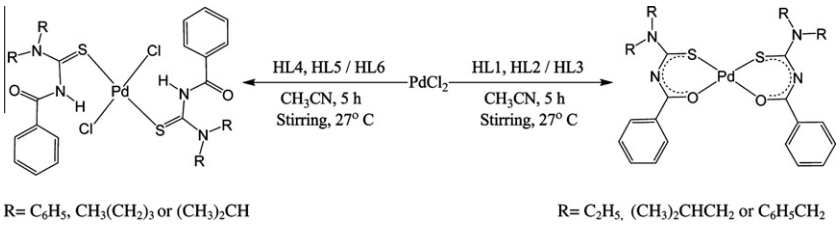

Scheme 1. Synthesis of palladium(II) complexes.

3.2. Electronic spectra

All the complexes are diamagnetic (μ_{eff} = 0) indicating +2 oxidation state of metal ion. The electronic spectra of all Pd(II) complexes were recorded in dichloromethane solution. Two bands were observed in the electronic spectra of **1**–**6** in the region 228–284 nm. These bands have been assigned to charge transfer transitions based on their very high molar extinction coefficient values (42 575–74 383 $dm^3\ mol^{-1}\ cm^{-1}$). This is in accord with other square planar Pd(II) complexes [51].

3.3. NMR spectra

In the ^{1}H NMR spectra of **1**, **2** and **3**, the characteristic signal at 11.25–11.95 ppm for N–H observed in the spectra of free ligands, disappeared, indicating deprotonation prior to coordination through enolization. By contrast, the resonance due to N–H was present around 11.30–11.95 ppm in the NMR spectra of **4**, **5** and **6**, indicating no enolization of ligands HL4, HL5 and HL6 and that they function as neutral ligand in **4**, **5** and **6**. Otherwise, the ^{1}H NMR spectra exhibited the expected resonances, multiplicity and integration consistent with the respective formulation. In the ^{13}C NMR spectra of all the complexes, carbonyl and thiocarbonyl carbon resonances were observed in the 170.3–178.2 and 163.4–172.1 ppm range respectively [6].

3.4. Crystal structures

The Pd atom in *cis*-[Pd(L1-O,S)$_2$] (**1**), is coordinated by two *N*,*N*-diethyl-*N*′-benzoylthiourea anions *via* the S and O atoms (Fig. 3). The Pd atom lies 0.0422(5) Å out of the least-square plane through the O_2S_2 donor atoms (rms deviation = 0.012 Å) which define an approximate square plane; each S atom is *trans* to an O atom. Each of the six-membered chelate ring is essentially planar with the rms for the six atoms defining S1-containing ring being only 0.065 Å (max. deviation = 0.069(1) Å for the O1 atom) compared to a rms of 0.134 Å for the second (max. deviation = 0.145(1) Å for the S2 atom) indicating a small distortion towards an envelope conformation; the dihedral angle formed between the two chelate rings is 1.80(5) Å. Each phenyl ring is effectively co-planar to the chelate ring to which it is connected as seen in the values of the O1–C6–C7–C8 and O2–C18–C19–C20 torsion angles of −179.25(16) and 5.8(2)°, respectively. Indeed, the only significant deviations from overall planarity in the molecule is found in the orientation of the *N*-bound ethyl groups with those connected to the N1 atom lying to the opposite side of the molecule compared to those bound to the N2 atom. Taken as a whole, the molecule of **1** approximates non-crystallographic twofold symmetry. There are two polymorphs of the uncoordinated HL1 ligand available in the literature [52,53] for comparison. Using the data of the most recent determination [53], it is salient to compare the formally C=S and C=O double bond distances of 1.67667(13) and 1.2188(14) Å, respectively, in HL1 with those given in Table 2. Evidently, there is significant elongation of these bonds in the complex. Further, the N–C bond distances of the chelate rings [N2–C1 1.345(2) and N2–C6 1.327(2) Å; N4–C13 1.345(2) and N4–C18 1.326(2) Å] have considerably shortened compared to the equivalent distances in HL1 of 1.4184(15) and 1.3868(15) Å, respectively. These results are consistent with deprotonation of HL1 during the reaction and significant delocalization of π-electron density over the six atoms comprising the respective chelate rings in the complex. The low temperature structure determination reported herein resolves literature ambiguities arising from disorder [6,7] and incorrect composition [52]. Molecules of *cis*-[Pd(L-O,S)$_2$] are consolidated in the crystal packing by C–H…π interactions[1] involving ethyl-H atoms interacting with the phenyl rings (Fig. 5) Globally, molecules form layers in the *ac*-plane and stack along the *b* axis being connected along that axis by C–H…π interactions involving the methylene-H2a atom and C19–C24 phenyl ring; the remaining interactions[1] contribute to the stability of the layers.

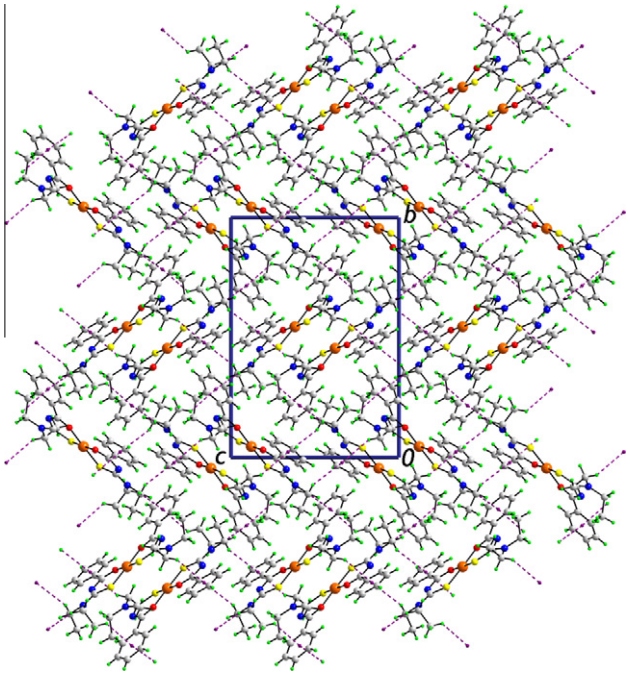

Fig. 5. Crystal packing diagram for **1** shown in projection down the *a* axis.

The Pd atom in *trans*-[PdCl$_2$(HL-S)$_2$] (**5**) is located on a center of inversion so that the *trans*-Cl_2S_2 donor set is planar (Fig. 4). Allowing for differences in the composition of the HL1 and HL5 ligands, the Pd-S bond distance in **5** is significantly longer than in **1** consistent with the S atom having more thione character in the former. This is also reflected in the significant shortening of the S1–C8 bond in **5** compared to the equivalent bonds in **1**. In the same way, the carbonyl bond is significantly shorter in **5**, consistent with its non-coordination. The molecular structure described herein for **5** resembles closely that reported for *trans*-[PdI$_2$(HL-S)$_2$] [54]. The

Table 2
Selected bond lengths (Å) and bond angles (°) for **1** and **5**.

1		**5**	
Pd–S1	2.2311(4)	Pd–Cl1	2.3070(9)
Pd–S2	2.2357(4)	Pd–S1	2.3178(8)
Pd–O1	2.0135(13)	S1–C8	1.710(3)
Pd–O2	2.0217(12)	O1–C7	1.214(4)
S1–C1	1.7376(18)		
S2–C13	1.7392(17)		
C6–O1	1.267(2)		
C18–O2	1.264(2)		
S1–Pd–S2	86.785(16)	Cl1–Pd–S1	85.52(3)
S1–Pd–O1	93.25(4)		
S1–Pd–O2	178.34(4)		
S2–Pd–O1	177.05(4)		
S2–Pd–O2	93.59(4)		
O1–Pd–O2	86.30(5)		

[1] Intermolecular C–H…π interactions operating in the crystal structure of *cis*-[Pd(L-O,S)$_2$]. Interactions between supramolecular layers: C2–H2a…Cg(C19-C24)^{i} = 2.86 Å, C2…Cg(C19-C24)^{i} = 3.738(2) Å, and angle at H2a = 149° for symmetry operation *i*: 3/2-*x*, -1/2 + *y*, 3/2-*z*. Interactions within supramolecular layers: C3–H3c…Cg(C19-C24)^{ii} 2.84 Å, 3.556(2) Å, 131° for *ii*: 1-*x*, 1-*y*, 1-*z*. C4–H4a…Cg(C7-C12)^{iii} 2.95 Å, 3.5135(19) Å, 117° for *iii*: 1-*x*, 1-*y*, 2-*z*. C14–H14a…Cg(C7-C12)^{ii} 3.00 Å, 3.6091(18) Å, 121°.

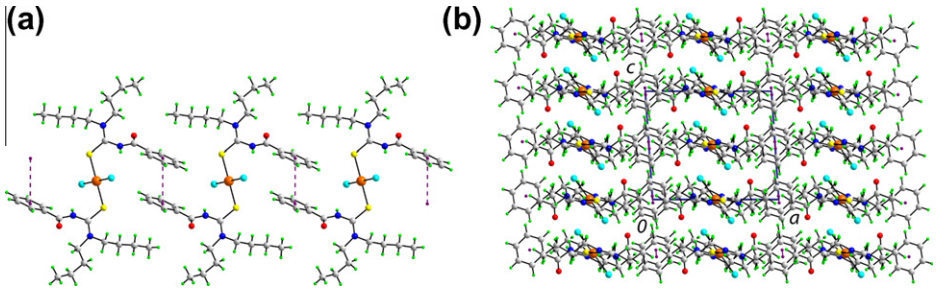

Fig. 6. Crystal packing diagram for **5** (a) supramolecular chain sustained by π...π interactions (shown as purple dashed lines) and (b) view of the stacking of layers along the *c*-axis. (For interpretation of the references to colour in this figure legend, the reader is referred to the web version of this article.)

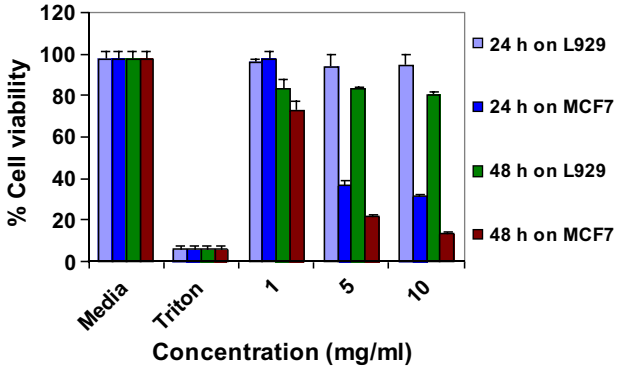

Fig. 7. Effect of **1** on the viability of breast cancer cells (all determinations are expressed as a percentage of the control).

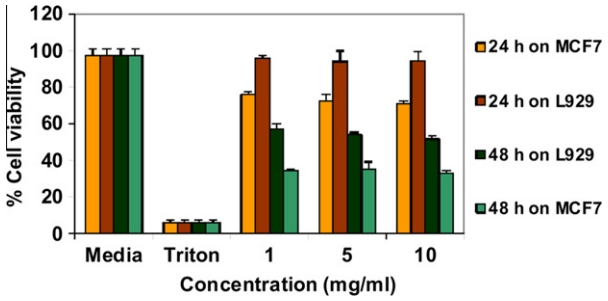

Fig. 8. Effect of **HL1** on the viability of breast cancer cells (all determinations are expressed as a percentage of the control).

observed molecular conformation in **5** is stabilized by an intramolecular N–H...Cl interaction.[2] As each of the S1, O1 and N1 atoms also forms a close intramolecular contact with a C–H atom,[2] the most important intermolecular interactions operating in the crystal structure are of the type π...π.[2] The latter lead to the formation of a supramolecular chain along the *a*-axis (Fig. 6a). Chains are arranged into layers in the *ab*-plane and stack along the *c*-axis (Fig. 6b).

3.5. Cytotoxicity studies

MTT assay was performed to evaluate the anticancer potential of complexes **1**–**6**. Only complex **1** showed significant activity against MCF7 cells and cytotoxicity of **1** was compared with that of ligand HL1. It is very evident that complex **1** at higher concentration (10 mg/ml) can inhibit the growth of MCF7 cells than at the lower concentrations of 1 and 5 mg/ml, whereas it did not affect the normal L929 cells even at higher concentration after 48 h (Fig. 7). HL1 was less toxic on MCF7 after 24 h (Fig. 8) but was enhanced after 48 h exposure. Compared to HL1, complex **1** was shown to be more toxic on MCF7 at a concentration of 5 and 10 mg/ml after 24 and 48 h. Higher cytotoxicity of complex **1** compared to HL1 suggests that the dual function approach that combines two biological mechanisms via single molecule significantly improves the biological activity of metal-based drugs [55]. Interestingly, complex **1** showed more than 80% cell viability after 48 h on L929 cells, indicating the possibility of specific toxicity to cancer cells. Cytotoxicity of **1** was compared with that of cispaltin. At higher concentrations (5 and 10 mg/ml) cisplatin showed higher toxicity compared to **1** whereas cytotoxicity of **1** was comparable with that of cisplatin at a concentration of 1 mg/ml [56].

4. Conclusion

Pd(II) complexes of *N*,*N*-di(alkyl/aryl)-*N*′-benzoylthiourea have been synthesized and characterized spectroscopically with two representative examples examined by X-ray crystallography. *N*,*N*-Di(alkyl/aryl)-*N*′-benzoylthiourea exhibited two different coordination modes with Pd(II). Eventhough the present ligands do not contain thiourea NH moiety, they are able to exhibit neutral monodentate coordination through the S atom in three complexes (**4**, **5**, and **6**). In remaining three complexes (**1**, **2** and **3**), *N*,*N*-di(alkyl/aryl)-*N*′-benzoylthiourea exhibited normal monobasic O,S bidentate coordination. One of the complexes (**1**) is cytotoxic to MCF cell lines.

Acknowledgements

N.S. acknowledges NITT for fellowship. The authors thank Dr. R. Jayakumar, Amrita Institute of Medical Sciences, Kochi, India for useful discussion on cytotoxicity studies. The authors also thank the University of Malaya for support of the crystallographic facility.

Appendix A. Supplementary material

CCDC 809545 and 809546 contain the supplementary crystallographic data for complexes **5** and **1**, respectively. These data can be obtained free of charge from The Cambridge Crystallographic Data Centre via www.ccdc.cam.ac.uk/data_request/cif. Supplementary data associated with this article can be found, in the online version, at doi:10.1016/j.ica.2011.06.031.

[2] Intra- and inter-molecular interactions in the crystal structure of *trans*-[$PdCl_2(HL\text{-}S)_2$]. Intramolecular: N1–H1...$Cl1^i$ = 2.43 Å, N1–H1...$Cl1^i$ = 3.114(3) Å and angle at H1 = 135° for symmetry operation *i*: 1-*x*, 1-*y*, 1-*z*; C9–H9a...N1 = 2.39 Å, C9–H9a...N1 = 2.811(4) Å and angle at H9a = 105°, C9–H9b...O1 = 2.52 Å, C9–H9b...O1 = 2.851(4) Å and angle at H9b = 100°; and C14–H14b...S1 = 2.79 Å, C14–H14b...S1 = 3.315(4) Å and angle at H14b = 115°. Intermolecular: ring centroid(C1-C6)...ring centroid$(C1\text{-}C6)^{ii}$ = 3.847(3) Å for *ii*: 2-*x*, 1-*y*, 1-*z*.

References

[1] N. Gunasekaran, R. Karvembu, Inorg. Chem. Commun. 13 (2010) 952.
[2] N. Gunasekaran, N. Remya, S. Radhakrishnan, R. Karvembu, J. Coord. Chem. 64 (2011) 491.
[3] R.A. Bailey, K.L. Rothaupt, Inorg. Chim. Acta 147 (1988) 233.
[4] W. Bensh, M. Schuster, Z. Anorg. Allg. Chem. 99 (1992) 611.
[5] D.J. Che, G. Li, X.L. Yao, Q.J. Wu, W.L. Wang, Y. Zhu, J. Organomet. Chem. 584 (1999) 190.
[6] M. Dominguez, E. Antico, L. Beyer, A. Aguirre, S. Garcia-Granda, V. Salvado, Polyhedron 21 (2002) 1429.
[7] G. Fitzl, L. Beyer, J. Sieler, R. Richter, J. Kaiser, E. Hoyer, Z. Anorg. Allg. Chem. 433 (1977) 237.
[8] R. Richter, L. Beyer, J. Kaiser, Z. Anorg. Allg. Chem. 461 (1980) 67.
[9] C. Sacht, M.S. Datt, S. Otto, A. Roodt, J. Chem. Soc., Dalton Trans. (2000) 727.
[10] R.D. Campo, J.J. Criado, R. Gheorghe, F.J. Gonzalez, M.R. Hermosa, F. Sanz, J.L. Manzano, E. Monte, E. Rodrıguez Fernandez, J. Inorg. Biochem. 98 (2004) 1307.
[11] W. Bensch, M. Schuster, Z. Anorg. Allg. Chem. 615 (1992) 93.
[12] H. Arslan, N. Kulcu, Transition. Met. Chem. 28 (2003) 816.
[13] K.R. Koch, Y. Wang, A. Coetzee, J. Chem. Soc., Dalton Trans. (1999) 1013.
[14] K.R. Koch, S. Bourne, J. Chem. Soc., Dalton Trans. (1993) 2071.
[15] Y.F. Yuan, J.T. Wang, M.C. Gimeno, A. Laguna, P.G. Jones, Inorg. Chim. Acta 324 (2001) 309.
[16] P.M. Shambula, M.J. Moloto, T.R. Tshikhudo, M. Fernandes, S. Afr. J. Sci. 106 (2010) 1.
[17] D.J. Che, X.L. Yao, G. Li, Y.H. Li, J. Chem. Soc., Dalton Trans. (1998) 1853.
[18] D.J. Che, X.L. Yao, G. Li, Y.H. Li, J. Chem. Soc., Dalton Trans. (1999) 2683.
[19] O. Seidelman, L. Beyer, R. Richler, Z. Naturforsch. 50B (1995) 1679.
[20] K.H. Konig, M. Schuster, B. Steinbrech, G. Schneeweis, R. Schlodder, Fresenius Z. Anal. Chem. 321 (1985) 457.
[21] P. Vest, M. Schuster, K.H. Konig, Fresenius Z. Anal. Chem. 335 (1989) 759.
[22] P. Vest, M. Schuster, K.H. Konig, Fresenius Z. Anal. Chem. 339 (1991) 142.
[23] P. Vest, M. Schuster, K.H. Konig, Fresenius Z. Anal. Chem. 341 (1991) 566.
[24] K.H. Konig, M. Schuster, G. Schneeweiss, B. Steinbrech, Fresenius Z. Anal. Chem. 319 (1984) 66.
[25] M. Schuster, E. Unterreitmeier, Fresenius Z. Anal. Chem. 346 (1993) 630.
[26] M. Schuster, M. Sandor, Fresenius Z. Anal. Chem. 356 (1996) 326.
[27] M. Schuster, E. Unterreitmeier, Anal. Chim. Acta 309 (1995) 339.
[28] M. Schuster, M. Schwarzer, Anal. Chim. Acta 328 (1996) 1.
[29] S.S. Rashid, N. Hussain, R. Ali, M. Jones, Eur. J. Med. Chem. 45 (2010) 323.
[30] S.S. Rashid, M. Jones, P.G. Hussain, R. Bhatti, Cent. Eur. J. Chem. 8 (2010) 550.
[31] S.S. Rashid, N. Jones, P.G. Yunus, J. Heterocycl. Chem. 47 (2010) 908.
[32] M. Eweis, S. Elkholy, S. Elsabee, M. Z. Int. J. Biol. Macromol. 38 (2006) 1.
[33] T.J. Egan, K.R. Koch, P.L. Swan, C. Clarkson, D.A. Van Schalkwyk, P. J. Smith. J. Med. Chem. 47 (2004) 2926.
[34] T. Rau, R. Van Eldik, in: A. Sigel, H. Sigel (Eds.), Metal Ions in Biological Systems, vol. 32, Marcel Dekker, New York, 1996, p. 339.
[35] W. Micklitz, W.S. Sheldrick, B. Lippert, Inorg. Chem. 29 (1990) 211.
[36] K.J. Barnham, C.J. Baucer, M.I. Djuran, M.A. Mazid, T. Rau, P.J. Sadler, Inorg. Chem. 34 (1995) 2826.
[37] W.Z. Shen, D. Gupta, B. Lippert, Inorg. Chem. 44 (2005) 8249.
[38] B. Lippert, Cisplatin: Chemistry and Biochemistry of a Leading Anticancer Drug, Wiley-VCH, Weinheim, Germany, 1999.
[39] T.A. AlAllaf, L. Rashan, J. Boll. Chim. Farmac. 140 (2001) 205.
[40] E.J. Gao, F.C. Liu, M.C. Zhu, L. Wang, Y. Huang, H.Y. Liu, S. Ma, Q.Z. Shi, N. Wang, Enzym. Inhib. Med. Chem. 25 (2010) 1.
[41] J. Ruiz, J. Lorenzo, L. Sanglas, N. Cutillas, C. Vicente, M.D. Villa, F.X. Aviles, G. Lopez, V. Moreno, J. Perez, D. Bautista, Inorg. Chem. 45 (2006) 6347.
[42] E.J. Goa, L. Wang, M.C. Zhu, L. Liu, W.Z. Zhang, Eur. J. Med. Chem. 45 (2010) 6347.
[43] E. Budzisz, M. Matecka, I.P. Lorenz, P. Mayer, R.A. Kwiecien, P. Paneth, U. Krajewska, M. Rozalski, Inorg. Chem. 45 (2006) 9688.
[44] J. Ruiz, M.D. Villa, N. Cutillas, G. Lopez, C.d. Haro, D. Bautista, V. Moreno, L. Valencia, Inorg. Chem. 47 (2008) 4490.
[45] J. Ruiz, J. Lorenzo, C. Vincente, G. Lopez, J.M. Lopez-de-Luzuriagu, M. Monge, F.X. Aviles, D. Bautista, V. Moreno, A. Laguna, Inorg. Chem. 47 (2008) 6990.
[46] R. Guddneppanavar, J.R. Choudhury, A.R. Kheradi, B.D. Steen, G. Saluta, G.L. Kucera, C.S. Day, U. Bierbach, J. Med. Chem. 50 (2007) 2259.
[47] H. Baruah, C.L. Rector, S.M. Monnier, U. Bierbach, Biochem. Pharmacol. 64 (2002) 191.
[48] G.M. Sheldrick, Acta Crystallogr., Sect. A 64 (2008) 112.
[49] L.J. Farrugia, J. Appl. Cryst. 30 (1997) 565.
[50] K. Brandenburg, DIAMOND, Crystal Impact GbR, Bonn, Germany, 2006.
[51] I.P. Romm, A.A. Malkov, S.A. Lebedev, V.V. Levashova, T.M. Buslaeva, Russ. J. Phys. Chem. A 85 (2011) 248.
[52] M. Bolte, L. Fink, Private Communication to the Cambridge Structural Database, 2003.
[53] L.R. Gomes, L.M.N.B.F. Santos, J.A.P. Coutinho, B. Schroder, J.N. Low, Acta Crystallogr., Sect. E 66 (2010) 870.
[54] K.R. Koch, S. Bourne, J. Mol. Struct. 441 (1998) 11.
[55] A. Valentini, F. Conforti, A. Crispini, A.D. Martino, R. Condello, C. Stellitano, G. Rotilio, M. Ghedini, G. Federici, S. Bernardini, D. Pucci, J. Med. Chem. 52 (2009) 484.
[56] Y. Min, C. Mao, D. Xu, J. Wang, Y. Liu, Chem. Commun. 46 (2010) 8424.